Mechanistic Mathematical Model for In Vivo Aroma Release during Eating of Semiliquid Foods

Ioan-Cristian Trelea, Samuel Atlan, Isabelle Déléris, Anne Saint-Eve, Michele Marin, Isabelle Souchon

Chemical Senses Advance Access published November 28, 2007

Chem. Senses doi:10.1093/chemse/bjm077

Mechanistic Mathematical Model for In Vivo Aroma Release during Eating of Semiliquid Foods

Ioan Cristian Trelea, Samuel Atlan, Isabelle Déléris, Anne Saint-Eve, Michèle Marin and Isabelle Souchon

UMR782 Génie et Microbiologie des Procédés Alimentaires, AgroParisTech, INRA, BP 01, 1 av. Lucien Brétignères, 78850 Thiverval-Grignon, France

Correspondence to be sent to: Ioan Cristian Trelea, UMR782 Génie et Microbiologie des Procédés Alimentaires, AgroParisTech, INRA, 1 av. Lucien Brétignères, 78850 Thiverval-Grignon, France. e-mail: cristian.trelea@agroparistech.fr

Abstract

The paper describes a mechanistic mathematical model for aroma release in the oropharynx to the nasal cavity during food consumption. The model is based on the physiology of the swallowing process and is validated with atmospheric pressure chemical ionization coupled with mass spectrometry measurements of aroma concentration in the nasal cavity of subjects eating flavored yogurt. The study is conducted on 3 aroma compounds representative for strawberry flavor (ethyl acetate, ethyl butanoate, and ethyl hexanoate) and 3 panelists. The model provides reasonably accurate time predictions of the relative aroma concentration in the nasal cavity and is able to simulate successive swallowing events as well as imperfect velopharyngeal closure. The most influent parameters are found to be the amount of the residual product in the pharynx and its contact area with the air flux, the volume of the nasal cavity, the equilibrium air/product partition coefficient of the volatile compound, the breath airflow rate, as well as the mass transfer coefficient of the aroma compound in the product, and the amount of product in the mouth. This work constitutes a first step toward computer-aided product formulation by allowing calculation of retronasal aroma intensity as a function of transfer and volatility properties of aroma compounds in food matrices and anatomophysiological characteristics of consumers.

Key words: APCI-MS, dynamic model, flavor release, mass transfer, swallowing physiology, yogurt

Introduction

During eating, aroma compounds initially present in the food matrix have to reach the olfactory epithelium by the retronasal pathway in order to be perceived by the consumer. The relationship between this release and the perception is quite complex and not well understood so far due, for example, to perceptual interactions and possibly to other poorly known mechanisms. It is therefore of a great interest to have a quantitative description of in vivo aroma release because 1) it is a key step in understanding the role of the product (composition and structure) and of the consumer (physiological parameters and individual experience) in the perceived flavor (Cook et al. 2005; Bult et al. 2007), 2) it is essential in understanding the role of the oral mechanisms and processes in the flavor release (Buettner et al. 2001), and 3) it could help to design food products taking physiological characteristics of individuals (young or elderly, healthy subjects, or with some clinical pathologies as dysphasia) into account. In this context, mechanistic models, describing the mass transfer of volatiles from food product to the air of the oral and nasal cavities, can constitute useful tool to predict aroma release and thus to identify the most important physicochemical, anatomical, and physiological parameters responsible for this release.

The development and the validation of such models require a better knowledge of both in vivo aroma concentrations and involved physiological mechanisms. The experimental determination of the aroma compound concentrations in the nasal cavity is now possible due to sufficiently sensitive and fast in vivo volatile measurement techniques such as atmospheric pressure chemical ionization (APCI-MS) or proton transfer reaction (PTR-MS) coupled with mass spectrometry. In the recent years, in vivo studies of volatile release using APCI-MS (e.g., Hodgson et al. 2004; Van Loon et al. 2005; Bayarri et al. 2006; King et al. 2006; Saint-Eve, Martin, et al. 2006) or PTR-MS (Hansson et al. 2003; Aprea et al. 2006; Boland et al. 2006) became more and more abundant. But the data

processing is often limited to computation of maximum intensities, slopes, areas, durations, and relative comparisons between these descriptors and if possible with sensory properties. The complexity of the olfactory system geometry (Damm et al. 2002) could explain the difficulty to establish a direct correlation between the volatile amount present in the nasal cavity and the one locally available for sensory receptors. Beyond quantification, the determination of the volatile release dynamic can constitute an important and useful step to better understand the dynamic of perception.

Detailed physiological studies of the deglutition process were performed by videofluoroscopy and real-time magnetic resonance imaging, giving a description of the key oral and pharyngeal stages of the swallowing act (Buettner et al. 2001). Some in vivo deglutition studies synchronously recorded a large number of physiological parameters: respiration by spirometry, mastication by electromyography, deglutition by electroglottography, and aroma compound release by APCI-MS (e.g., Hodgson et al. 2003). Such synchronous studies are particularly valuable because they allow the integration of the various signals in an overall mechanistic picture. For instance, lots of authors agreed to establish a direct link between volatile apparition in the nasal cavity and swallowing events (Buettner et al. 2002; Hodgson et al. 2003), but, because of the interindividual variability and the complexity of the consumption and perception processes, few studies developed an integrated modeling approach taking into account the whole physiological, physicochemical, and kinetic phenomena.

The development of a dynamic release model consists in the calculation of the amounts of aroma compounds transferred from the food matrix to the nasal cavity in the course of the eating process. Pioneering work in flavor-release modeling during food consumption is due to Harrison et al. (Harrison 1998; Harrison et al. 1998). A theoretical description of aroma release was proposed on the basis of mass transfer theory, but these models did not include experimental validation and made strong simplifying assumptions, like constant breath airflow, which are relatively far from reality. Based on these first in vivo modeling attempts, improvements of flavor-release models have been proposed by integrating a more realistic description of physiological mechanisms: 1) mastication for semisolid products as sweet gel (Wright and Hills 2003; Wright, Sprunt, et al. 2003) and 2) flow in the throat for liquids (Wright, Hills, et al. 2003). The flavor persistence was quite well represented by this last model, but the signal intensity in the first breath was not in agreement with in vivo experiments. Based on the empirical approach suggested by Linforth and Taylor (2000), Linforth et al. (2002) have used a quantitative structure property relationships method to represent flavor release from solutions after the first 2 swallowing events. In the case of a semisolid product (gelled emulsion particles), Lian et al. (2004) have modeled flavor release and underlined the important role of the product structure on the main mechanisms explaining the release. Their mathematical model was focused more on the product than on the physiological conditions during eating process. Normand et al. (2004) developed a volatile release model from liquid products based on a simplified but realistic description of the human swallowing and breathing process. Distinct mechanisms were assumed for the first breath after the deglutition event and the subsequent ones. Short-time persistence (less than 1 min) of the aroma release was considered to be mainly due to saliva coating, whereas longer time persistence to volatile adsorption in the mucosa. All these studies constituted a real progress in analyzing aroma release, but they illustrated the need for a better integration of the complexity of the involved phenomena to describe more realistically aroma release.

The present work focuses on modeling in vivo aroma release from semisolid (gelled) food matrices. The model is based on anatomic and physiologic reality of the swallowing process and describes volatile release without distinction between the first and the subsequent breaths. Validation is performed by comparing simulations with in vivo APCI-MS volatile measurements. This model intends to be a step toward quantitative mechanistic description of the retronasal olfactory stimulus generation. Possible applications include computer-aided product formulation, considering the retronasal aroma intensity as a function of aroma compound properties in food matrices and anatomophysiological characteristics of the consumers.

Materials and methods

Measurement of volatiles concentration in the nasal cavity

The concentration of the volatile compounds in the nasal cavity of the panelists was measured by APCI-MS using an Esquire-Liquid Chromatograph mass spectrometer (Bruker Daltonique, Wissenbourg, France) as previously described (Saint-Eve, Martin, et al. 2006). Air was sampled from the subject's nose at a flow rate of 35 ml/min through a deactivated fused silica tubing (Supelco, Saint Quentin Fallavier, France). A glass Y junction was set up between the entry of the APCI-MS capillary and the subject's nose. The protonated molecular ion of each target molecule was detected at its corresponding m/z value, indicated in Table 1. In addition to the 3 esters considered in this study, the acetone signal (m/z = 59) was also recorded, as a marker of subject's breath. Acetone is naturally produced by human liver and is present in the air expired from the lungs (Wilson 1986) at a concentration that was assumed constant for the duration of the experiments (less than 2 min). In order to attenuate the measurement noise, the APCI-MS signals stored at a rate of 10 samples per second were filtered by a symmetric moving average filter with a ±1-s time window and 1 filtered value per second was retained. The stability of the APCI-MS signal was checked with a reference gas (headspace of a solution of heptan-2-one at 15 parts per million) before and after the

Table 1 Model parameter values

Parameter	Symbol	Value
Volumes of the compartments (cm^3)		
Product in oral cavity (max)	V_{OPM}	5
Product in oral cavity (min)	V_{OPm}	0.77
Air in oral cavity (max)	V_{OAM}	5
Air in oral cavity (min)	V_{OAm}	0.05
Residual product in the pharynx	V_{FP}	0.1
Air in the pharynx (max)	V_{FAM}	50
Air in the pharynx (min)	V_{FAm}	0.5
Air in the nasal cavity	V_{NA}	320
Contact areas (cm^2)		
Air/product in the oral cavity	A_{OAP}	215
Air/product in the pharynx	A_{FAP}	66
Pharynx/oral cavity (air, max)	A_{FOAM}	5
Mass transfer coefficients (cm/s)		
In the product (product/air interface)	k_P	$3\cdot\times 10^{-4}$
In the air (product/air interface)	k_A	3
In the air (pharynx/oral cavity communication)	k_{FOA}	1.5
Air/product equilibrium partition coefficients at 20 °C (g/g)		
Ethyl acetate, CAS yogurt	K_{AP}	7.31×10^{-3}
Ethyl acetate, MPO yogurt	K_{AP}	$7.38\cdot\times 10^{-3}$
Ethyl butanoate, CAS yogurt	K_{AP}	$5.67 \times\cdot 10^{-3}$
Ethyl butanoate, MPO yogurt	K_{AP}	5.75×10^{-3}
Ethyl hexanoate, CAS yogurt	K_{AP}	0.83×10^{-3}
Ethyl hexanoate, MPO yogurt	K_{AP}	1.07×10^{-3}
Flow rates (cm^3/s)		
Saliva	Q_S	0.1
Respiration	Q_R	−500 to 500
Duration of the deglutition steps (s)		
Step 1: product residence in the mouth	τ_1	10 to 60
Step 2: contraction of the oral cavity	τ_2	0.2
Step 3: contraction of the oral cavity and of the pharynx	τ_3	0.3
Step 4: relaxation of the oral cavity and of the pharynx	τ_4	0.3
Initial concentrations of the aroma compounds in the product ($\mu g/cm^3$)		
Ethyl acetate (m/z = 89)	C_{OP0}	18
Ethyl butanoate (m/z = 117)	C_{OP0}	27
Ethyl hexanoate (m/z = 145)	C_{OP0}	22

release experiments. Relative aroma compound concentrations were determined as ratios of APCI peak heights at the corresponding m/z values.

Preparation of the flavored products

Two flavored stirred yogurts were used in this study. Their preparation and properties were previously described in detail (Saint-Eve, Levy, et al. 2006). They had the same dry matter (22.5%), fat (4%), and total protein (5.4%) contents, but different protein fractions: yoghurt enriched with sodium caseinate (CAS) (complex viscosity at 0.1 Pa: 159 Pa·s), whereas yoghurt enriched with milk powder (MPO) (complex viscosity at 0.1 Pa: 109 Pa·s). Yogurts were flavored to 1 mg/g with a strawberry flavor containing 17 aroma compounds mixed with propylene glycol (Saint-Eve, Levy, et al. 2006). The compounds considered in this study were ethyl acetate, ethyl butanoate, and ethyl hexanoate, whose initial concentrations in the yogurt (C_{OP0}) are given in Table 1.

Yogurt consumption protocol

The yogurt consumption protocol was organized as described by Saint-Eve, Martin, et al. (2006). During a session, each of the 3 panelists considered in this study ate 5 cm^3 of yogurt at 10 °C. They had to keep the yogurt in the mouth for 12 s and to swallow. Then, they had to continue eating normally. The nose-space APCI-MS signal was recorded for at least 1 min after having introduced the yogurt in the mouth. The swallowing events during this time were recorded. Each experiment was repeated 4 times.

Estimation of the instantaneous breath flow rate

The breath flow rate of the panelists during the consumption of flavored products was estimated from the acetone signal measured in the nasal cavity and recorded synchronously with the concentration of the target aroma compounds. During inspiration, the acetone concentration in the nasal cavity decreases due to dilution by ambient air, whereas during expiration, it increases due to the contribution of the air coming from the lungs. The instantaneous breath flow rate was thus estimated as being proportional to the (minus) derivative of the acetone concentration signal. The proportionality factor, necessary for scaling the flow rate in physical units, was obtained from spirometric data recorded for each panelist during 1 min before each experiment (spirometer PulmoSystem 2, Datalink, MSR, Paris, France).

Mathematical model

Principle of the developed model

Before presenting the equations describing flavor transfer occurring in the yogurt-eating process, the principle and the main steps of the developed model are described first. The

purpose of this section is to give an outline of the modeling approach without going into any mathematical detail. The starting point for developing the mechanistic model is a physiological representation of the deglutition process. Volatile release is quantitatively described using tools from chemical engineering. The various parts of the upper respiratory tract are viewed as interconnected reactors, containing an air phase and possibly a flavored product phase. The deglutition process is decomposed into 4 main steps. Detailed mass balances are written for each step in each compartment. Mass balances include volatile release at air–product interface and, when appropriate, bulk flows for product and air.

When air and product phases are in contact, volatile transfer occurs across the interfacial layers (Figure 1). On each side of the interface, the driving force is the concentration difference between the bulk phase and the interface. At the infinitely thin interface, local equilibrium is expressed via the partition coefficient between phases. The released volatile flux also depends on the contact area between phases and on the transfer resistance in each phase, expressed via mass transfer coefficients. In addition to interfacial release, bulk flow may also occur between various compartments. In this case, volatile mass balances directly involve bulk concentrations and bulk flow rates.

In the model, the above mass transfer mechanisms are used according to the adopted physiological description of the deglutition process. When the mouth is closed, the oral cavity is generally isolated from the upper airway and the subjects breathe normally. The main phenomena are volatile release from product to the air in the oral cavity and product dilution by saliva. Some aroma release to the pharynx and further to the nasal cavity is possible, however, for panelists with imperfect velopharyngeal closure. At the beginning of the swallowing reflex, breathing is stopped and oral cavity contraction expels aroma-rich air. Further oral and pharynx contraction allows product swallowing, that is, reduction of the amount of the product in the mouth and coating of the pharynx by a thin product film. At the end of the swallowing reflex, the oral cavity and the pharynx are distended and filled with air. The subject starts breathing again and a new cycle begins. An important change occurs, however, after the first deglutition event: the aromatized product film coating the pharynx is permanently in contact with the breath airflow, inducing continuous aroma release to the nasal cavity.

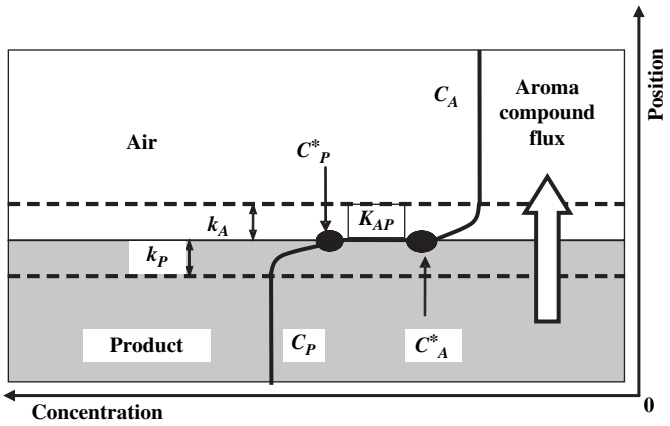

Figure 1 Schematic representation of the aroma compound concentration near the product–air interface. In each phase, the concentration is assumed essentially uniform, except in a thin interfacial layer. The concentration profile appears discontinuous at the interface due to air/product partition properties.

These qualitative considerations on the aroma release during the eating process were translated into a quantitative model as described in detail below.

Detailed mathematical model description

In order to quantify aroma compound release during food consumption, the oral cavity (index O), the pharynx (index F), and the nasal cavity (index N) were described as interconnected perfectly mixed reactors containing a product phase (index P) and/or an air phase (index A). A schematic representation of these compartments, together with their connections with the ambient air, the esophagus, and the trachea is given in Figure 2. The airflow rates were arbitrarily considered to be positive if their direction is the one indicated by the arrows in Figure 2 (inspiration) and negative in the opposite case (expiration). Aroma compound concentrations in all compartments were calculated using mass balances. In order to limit model complexity, heat transfer was not modeled explicitly, that is, isothermal conditions were assumed. It was verified in separate experiments that, after introduction of the cold yogurt in the mouth, product and mouth quickly reached a common temperature close to 20 °C, which remained essentially constant for the duration of the release experiment.

For modeling purposes, the process of product consumption was assumed to be a succession of deglutition cycles, each one being divided in 4 steps, based on human physiology as described by Buettner et al. (2001). The steps were defined in such a way as to ensure a cyclic model operation, that is, the final state at the end of step 4 becomes the initial state of the step 1 in the following deglutition cycle. The first step of the first cycle started as soon as the product was introduced and the mouth was closed.

Step 1: product residence in the mouth

During this step (duration: τ_1), the mouth is closed and the subjects breathe normally, according to the experimental protocol. The volumes of all compartments are constant and equal to their maximum (distended) values. The only exception is the volume of the product in the oral cavity (V_{OP}), which is diluted by the saliva flow (Q_S):

$$\frac{dV_{OP}}{dt} = Q_S. \tag{1}$$

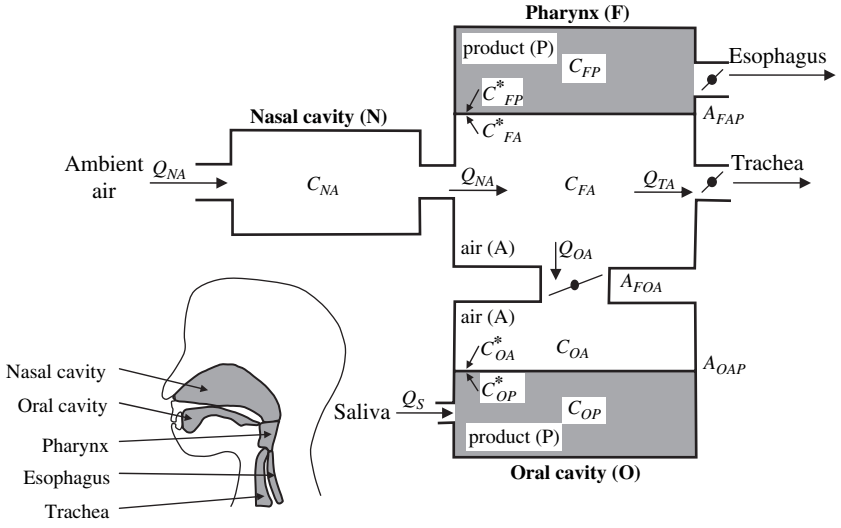

Figure 2 Schematic representation of the nasal cavity, pharynx, and oral cavity as interconnected reactors. Oral cavity (index O), pharynx (index F), nasal cavity (index N), product phase (index P), and air phase (index A). The airflow rates are formally considered to be positive if their direction is the one indicated by the arrows (inspiration) and negative in the opposite case (expiration).

There is no airflow in the oral cavity ($Q_{OA} = 0$), and the airflow through the nasal cavity (Q_{NA}) is equal to that in the trachea (Q_{TA}):

$$Q_{TA} = Q_{NA}, \quad Q_{OA} = 0. \tag{2}$$

The main phenomena responsible for the variation of the aroma concentration in the product present in the oral cavity (C_{OP}) are dilution by the saliva flow and transfer through the product–air interface (area: A_{OAP}):

$$\frac{dC_{OP}}{dt} = \frac{Q_S}{V_{OP}}(0 - C_{OP}) + k_P\frac{A_{OAP}}{V_{OP}}(C^*_{OP} - C_{OP}) \tag{3}$$

It was assumed in this equation that fresh saliva has null concentration in the considered aroma compound and that the mass transfer coefficient between the interfacial layer of the product (interfacial concentration on the product side C^*_{OP}) and the bulk (concentration C_{OP}) has value k_P.

The air in the oral cavity (concentration C_{OA}) receives aroma compounds from the product (interfacial concentration on the air side C^*_{OA}, mass transfer coefficient k_A). In addition, the air in the oral cavity may exchange volatile molecules with the air in the pharynx (concentration C_{FA}) if there is an imperfect velopharyngeal closure. Provision was taken in the model for this possible oral-pharynx volatile transfer by considering a time-varying oropharynx contact area (A_{FOA}). Perfect closure is thus denoted by $A_{FOA} = 0$. A mass transfer coefficient between the oral cavity and the pharynx (k_{FOA}) was formally introduced to account for the transfer resistance:

$$\frac{dC_{OA}}{dt} = k_A\frac{A_{OAP}}{V_{OA}}(C^*_{OA} - C_{OA}) + k_{FOA}\frac{A_{FOA}}{V_{OA}}(C_{FA} - C_{OA}). \tag{4}$$

The interfacial aroma compound concentrations on the product side (C^*_{OP}) and on the air side (C^*_{OA}) were calculated using the mass flux conservation and the partition conditions at the interface (Cussler 1997):

$$k_P A_{OAP}(C^*_{OP} - C_{OP}) + k_A A_{OAP}(C^*_{OA} - C_{OA}) = 0, \tag{5}$$

$$\frac{C^*_{OA}}{C^*_{OP}} = K_{AP}, \tag{6}$$

where K_{AP} is the apparent air/product partition coefficient. Equations (5) and (6) were solved for the interfacial concentrations (C^*_{OA} and C^*_{OP}).

The air in the pharynx (concentration C_{FA}) exchanges aroma compounds with the residual product coating the pharynx walls (interfacial concentration on the air side C^*_{FA}), with the air in the oral cavity (concentration C_{OA}) as described above and is also diluted by the respiration air flux. The respiration air flux (Q_{NA}) comes either from the nasal cavity with concentration C_{NA} during inspiration ($Q_{NA} \geq 0$) or from the trachea during expiration ($Q_{TA} = Q_{NA} < 0$). The air coming from the trachea was assumed to be aroma free because of the strong preference of the aroma compounds for the aqueous phase ($K_{AP} \ll 1$, meaning that the aroma compounds present in the inspired air are quickly absorbed into the lungs) and of the very high contact area of the lungs ($\sim 100\ m^2$). With these considerations, the concentration of the aroma compound in the air contained in the pharynx (C_{FA}) was expressed as

$$\frac{dC_{FA}}{dt} = k_A\frac{A_{FAP}}{V_{FA}}(C^*_{FA} - C_{FA}) + k_{FOA}\frac{A_{FOA}}{V_{FA}}(C_{OA} - C_{FA}) + \begin{cases} \frac{Q_{NA}}{V_{FA}}(C_{NA} - C_{FA}), & \text{if } Q_{NA} \geq 0, \\ \frac{-Q_{TA}}{V_{FA}}(0 - C_{FA}), & \text{if } Q_{NA} < 0. \end{cases} \tag{7}$$

The residual product in the pharynx (concentration C_{FP}) exchanges aroma compounds with the adjacent air (interfacial concentration on the product side C^*_{FP}):

$$\frac{dC_{FP}}{dt} = k_P \frac{A_{FAP}}{V_{FP}}(C^*_{FP} - C_{FP}). \quad (8)$$

Before the first swallowing event, there is no product present in the pharynx, but the pharynx walls are coated with saliva (initially aroma free). During this time, C_{FP} represents the concentration in the saliva film, allowing equations (7) and (8) to be written in the same way as for subsequent swallowing cycles.

The interfacial aroma compound concentrations on the product (C^*_{FP}) and on the air side in the pharynx (C^*_{FA}) were calculated similarly to the oral cavity, that is, using equations (5) and (6) with index F (pharynx) replacing the index O (oral cavity).

Finally, the concentration of the aroma compound in the nasal cavity (C_{NA}) results from mixing with the breath air flux. The ambient air coming during inspiration ($Q_{NA} \geq 0$) is assumed aroma free, whereas during the expiration ($Q_{NA} < 0$) air with concentration (C_{FA}) comes from the pharynx:

$$\frac{dC_{NA}}{dt} = \begin{cases} \frac{Q_{NA}}{V_{NA}}(0 - C_{NA}), & \text{if } Q_{NA} \geq 0, \\ \frac{-Q_{NA}}{V_{NA}}(C_{FA} - C_{NA}), & \text{if } Q_{NA} < 0. \end{cases} \quad (9)$$

Step 2: contraction of the oral cavity (air expulsion)

This step (duration: τ_2) corresponds to the beginning of the swallowing reflex. The volume of the air in the oral cavity (V_{OA}) is reduced from its initial maximum value (V_{OAM}) to some small residual amount (V_{OAm}), resulting in expulsion of aroma-rich air to the pharynx and further to the nasal cavity:

$$\frac{dV_{OA}}{dt} = \frac{V_{OAm} - V_{OAM}}{\tau_2} < 0. \quad (10)$$

Communication with the trachea is closed. The air flux to the trachea (Q_{TA}) is zero, and the air flux from the oral cavity to the pharynx (Q_{OA}) and further to the nasal cavity (Q_{NA}) is due to the volume reduction:

$$Q_{TA} = 0, \quad Q_{OA} = Q_{NA} = \frac{dV_{OA}}{dt} < 0. \quad (11)$$

The volume of the product in the oral cavity (V_{OP}) is still given by equation (1). For the product in the oral cavity (concentration C_{OP}), the mass transfer phenomena are identical to step 1 and are given by equation (3). The expression of the aroma concentration in the air of the oral cavity (C_{OA}) is similar to equation (4) except that the term corresponding to transfer with the pharynx is missing due to the presence of the bulk airflow:

$$\frac{dC_{OA}}{dt} = k_A \frac{A_{OAP}}{V_{OA}}(C^*_{OA} - C_{OA}). \quad (12)$$

The evolution of the air concentration in the pharynx (C_{FA}) is given by equation (13), which is similar to equation (7) except that the dilution by the breath air is missing, and the transfer term with the oral cavity is replaced by dilution due to expulsed air:

$$\frac{dC_{FA}}{dt} = k_A \frac{A_{FAP}}{V_{FA}}(C^*_{FA} - C_{FA}) + \frac{-Q_{OA}}{V_{FA}}(C_{OA} - C_{FA}) \quad (13)$$

The aroma concentration in the residual product in the pharynx (C_{FP}) is still given by equation (8). The concentration in the nasal cavity (C_{NA}) results from mixing the air coming from the pharynx. It is given by equation (9) taking into account that the air flux is always negative ($Q_{NA} < 0$) in step 2 (eq. 11).

Step 3: contraction of the oral cavity and of the pharynx (product swallowing)

During this step (duration: τ_3), the pharynx is contracted, expulsing the air to the nasal cavity. The volume of the air in the pharynx (V_{FA}) is reduced from its initial maximum value (V_{FAM}) to some small residual amount (V_{FAm}):

$$\frac{dV_{FA}}{dt} = \frac{V_{FAm} - V_{FAM}}{\tau_3} < 0. \quad (14)$$

The oral cavity contracts further, pushing the bolus to the esophagus via the pharynx. The volume of the product in the oral cavity (V_{OP}) is reduced from its value reached at the end of step 2 (V_{OP2}) to a small residual value (V_{OPm}):

$$\frac{dV_{OP}}{dt} = \frac{V_{OPm} - V_{OP2}}{\tau_3} < 0. \quad (15)$$

The other volumes remain constant during this step. The air flows to the trachea (Q_{TA}) and to the oral cavity (Q_{OA}) are zero, whereas the air flow from the pharynx to the nasal cavity (Q_{NA}) is due to the volume reduction:

$$Q_{TA} = 0, \quad Q_{OA} = 0, \quad Q_{NA} = \frac{dV_{FA}}{dt} < 0. \quad (16)$$

In addition to the airflows, a product flow (Q_{OP}) appears in step 3, due to the contraction of the oral cavity. This product flow also includes the saliva flow, which is assumed to be constant in time:

$$Q_{OP} = \frac{dV_{OP}}{dt} - Q_S < 0. \quad (17)$$

The concentrations of the considered aroma compound in the product contained in the oral cavity (C_{OP}) and in the air of the oral cavity (C_{OA}) are given by equations (3) and (12), respectively. The concentration in the air contained in the pharynx (C_{FA}) is given by equation (18), which is similar to equation (13) except that the dilution term is missing:

$$\frac{dC_{FA}}{dt} = k_A \frac{A_{FAP}}{V_{FA}}(C^*_{FA} - C_{FA}). \quad (18)$$

Concerning the product in the pharynx (concentration C_{FP}), an additional mixing term appears in this step compared with

equation (8) due to the product flow from the oral cavity through the pharynx to the esophagus:

$$\frac{dC_{FP}}{dt} = k_P \frac{A_{FAP}}{V_{FP}}(C^*_{FP} - C_{FP}) + \frac{-Q_{OP}}{V_{FP}}(C_{OP} - C_{FP}). \quad (19)$$

The concentration in the nasal cavity (C_{NA}) is given by equation (9) taking into account that the airflow is always negative ($Q_{NA} < 0$) in step 3 (eq. 16).

Step 4: relaxation of the oral cavity and of the pharynx (air influx)

Step 4 of the product consumption cycle (duration: τ_4) corresponds to the relaxation of the oral cavity and the pharynx. The trachea is still closed in this step. The air compartments are filled with air coming from the nasal cavity. The volume of the air in the oral cavity (V_{OA}) increases from its minimal (V_{OAm}) to its maximal values (V_{OAM}):

$$\frac{dV_{OA}}{dt} = \frac{V_{OAM} - V_{OAm}}{\tau_4} > 0. \quad (20)$$

The expression for the air volume in the pharynx (V_{FA}) is similar, replacing index O with index F in equation (20). The air inflow in the oral cavity (Q_{OA}) is due to the oral volume increase. The airflow from the nasal cavity (Q_{NA}) additionally includes pharynx volume increase (Figure 2):

$$Q_{OA} = \frac{dV_{OA}}{dt} > 0, \quad Q_{NA} = Q_{OA} + \frac{dV_{FA}}{dt} > 0. \quad (21)$$

The volume of the product in the oral cavity (V_{OP}) is given by equation (1), and the other volumes are constant.

After the end of step 4, calculations continue cyclically with step 1. The model state at the end of step 4 (volumes and aroma compound concentrations in the various compartments) becomes the initial state for the new cycle.

Model simulation and parameters

The starting time for the model simulation ($t = 0$) is the moment when the panelist introduces the product in the oral cavity and closes the mouth. At the initial time, all time-varying volumes (product in the oral cavity and air in the oral cavity and in the pharynx) have their maximum values (eq. 22). The concentration of the aroma compound in the product (C_{OP}) is equal to the amount introduced during the product preparation, whereas all other compartments shown in Figure 2 are aroma free (eq. 23):

$$V_{OP}(0) = V_{OPM}, \quad V_{OA}(0) = V_{OAM}, \quad V_{FA}(0) = V_{FAM}, \quad (22)$$

$$C_{OP}(0) = C_{OP0}, \quad C_{OA}(0) = 0, \quad C_{FA}(0) = 0,$$
$$C_{FP}(0) = 0, \quad C_{NA}(0) = 0. \quad (23)$$

In each of the 4 steps of the deglutition process mentioned above, model simulation requires the simultaneous solution of 12 coupled equations: 8 ordinary differential equations (3 for the time-varying volumes, 5 for the bulk aroma compound concentrations) and 4 algebraic equations for the interfacial concentrations. These equations were solved numerically using the Matlab 7 simulation software (The MathWorks, Natick, MA).

The parameter values required for model simulation are listed in Table 1. These parameters are related either 1) to the product (e.g., initial aroma compound concentrations, air/product equilibrium partition coefficients), 2) to the consumer anatomy and physiology (such as the volumes of the compartments, saliva and airflow rates, durations of the various steps of the deglutition process), or 3) to the interaction of both (e.g., residual amounts of the product, mass transfer coefficients, and product–air contact areas are expected to depend both on product rheology and on the mouth and pharynx configuration and movement). The values for these parameters were selected as explained below.

The initial concentrations of the aroma compounds in the product were given by the product flavoring protocol, as described in the experimental section. The air/product partition coefficients K_{AP} were measured specifically for each aroma compound/product couple by the nonlinear phase ratio variation technique (Ettre et al. 1993; Atlan et al. 2006). The volume of the product introduced in the oral cavity V_{OPM} was fixed by the experimental protocol to 5 cm^3 (volume contained in a spoon) and corresponded to a realistic amount, even if one can notice a wide range of values used in swallowing studies (Shaw et al. 2004; Linforth et al. 2005; Stephen et al. 2005; Seta et al. 2006).

Concerning the physiological parameters, the total free volume of the oral cavity was estimated at about 10 cm^3 by spit-out experiments with water, in accordance with literature data (Lauder and Muhl 1991; Kahrilas et al. 1993). The maximum air volume V_{OAM} was taken as the difference with the product volume. The residual (minimum) air volume in the oral cavity V_{OAm} was arbitrarily set to 1/100 of this value. The pharynx geometry (maximum volume, surface area, and contact area with the mouth) was estimated using an anatomic atlas (Netter 2004), and literature data obtained by biplane videofluoroscopy (Kahrilas et al. 1993). The volume of the nasal cavity V_{NA} was set to a typical value according to Damm et al. (2002), even if very high interindividual variations were observed. Hodgson et al. (2003) also specified that volume of the retronasal pathway involved in aroma release could be different depending on the process (swallowing or mastication). The saliva flow rate Q_S was measured at rest for the considered panelists and fixed to an average value. The duration of the first step (τ_1) of the product consumption cycle was determined in each case by recording the swallowing events. The durations of the other deglutition steps (τ_2, τ_3, and τ_4 for steps 2, 3, and 4, respectively) were estimated by considering the description of the physiology of swallowing (Buettner et al. 2001) and the total duration of a swallowing act (Hiss et al. 2001) and were in agreement with the data of Dodds (1989) and Kahrilas et al. (1993).

As regards parameters dependent on both the product and the eating process, the surface area of the mouth A_{OAP}, and the residual product volume in the mouth after deglutition V_{OPm} were measured by Collins and Dawes (1987). Bogaardt et al. (2007) estimated the residual volume of product in the pharynx (V_{FP}) to about 2% of the initial volume introduced in mouth (which would give 0.1 cm^3 here) and highlighted that it was weakly dependent on product viscosity. We initially estimated this parameter (V_{FP}) at 0.3 cm^3 by assuming a similar amount per unit area as in the mouth (Collins and Dawes 1987). It was then reduced to 0.1 cm^3 to account for the observed aroma persistence signal. This seems reasonable taking into account the lack of "dead" volumes in the pharynx as compared with the ones in mouth (between teeth, under the tongue, etc.). The interfacial mass transfer coefficients in the product (k_P) and in the air (k_A and k_{FOA}) are known to have relatively similar values for various molecules and were set to usual values according to Marin et al. (1999) and Cussler (1997).

It should be noted, however, that most of these parameters are subject to strong interindividual variations and are in many cases only crude estimations. The effects of these parameters on model predictions were examined as described in the Results in order to determine those on which additional experimental efforts should be concentrated.

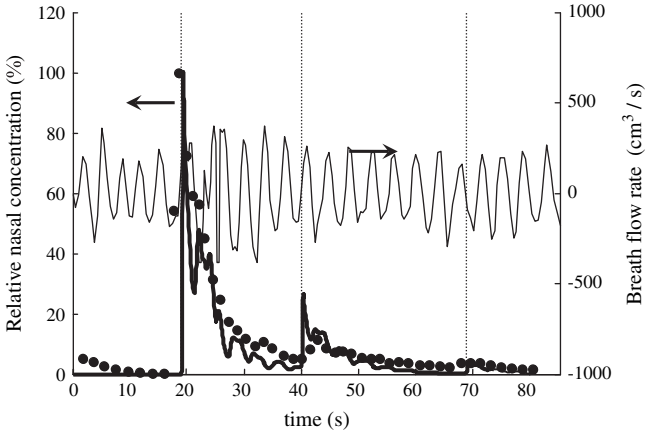

Figure 3 Example of model validation in a typical situation. Release of ethyl acetate in the nasal cavity of panelist A during the consumption of CAS yogurt. Measured (•) and simulated (— bold) relative aroma compound concentration in the nasal cavity, breath flow rate (— thin), and deglutition events (|).

Results

Typical results

With the considered experimental setup, the only model prediction that could be validated against measured data was the relative concentration of the target aroma compounds in the nose space of the subjects. This concentration was considered because of its relevance to aroma perception. A typical result of a model simulation is shown in Figure 3. Agreement with the measured nose-space concentration is reasonably good, taking into account the simplifying modeling assumptions versus the complexity of the oropharynx anatomy and of the swallowing physiology. It is worth noticing that similar adequacy between experimental release kinetics in the nasal cavity and model simulations was observed for all panelists, aroma compounds, and products studied. It appears in Figure 3 that aroma compound concentration in the nasal cavity of the subject is very low before the first deglutition event (step 1 of the model), denoting almost perfect closure of the velopharynx while the product is kept in the mouth (for this particular experiment). A sharp increase of this concentration occurs immediately after the first swallow: both the expulsion of an aroma-rich air from the oral cavity (step 2) and the quick increase of the volatile concentration in the pharynx due to the product flow toward the esophagus (step 3) can explain this release peak. The aroma concentration in the nasal cavity gradually decreases until the next deglutition event: the small residual amount of the product present in the pharynx continues to release aroma compound but this concentration is continuously diluted by the airflow (Normand et al. 2004). Subsequent swallows increase aroma concentration in the nasal cavity but to a much lesser extent than the first swallow because of the residual product dilution by the saliva in the oral cavity.

To illustrate the way the model integrates the considered physiological and mass transfer mechanisms, representation of additional calculated variables is given in Figure 4. The product volume in the oral cavity (V_{OP}) (Figure 4A) gradually increases between swallows due to permanent saliva flow and decreases abruptly to a small residual value at each swallowing time. The saliva flow also induces the dilution of the aroma compound in the product: its concentration (C_{OP}) decreases slowly when the amount of the product is high and faster after each swallow, when the total amount of the product becomes smaller (Figure 4C). The air volume in the oral cavity V_{OA} is essentially constant, except during the contraction of the oral cavity in the swallowing reflex (Figure 4B). The air volume in the pharynx has similar variations (data not shown). The volatile concentration in the air contained in the oral cavity (C_{OA}) increases between swallows due to mass transfer from the product to the gaseous phase and decreases quickly immediately after the swallows because of the fresh air intake during the relaxation of the oral cavity (Figure 4D). The aroma compound concentration in the product present in the pharynx (C_{FP}) is null before the first swallowing event. The flow of aroma-rich product from the mouth at each swallow induces a sharp increase in this concentration (Figure 4E). Between swallows, this concentration decreases gradually, the volatile compound being transferred from the product toward the air and swept out by the breath airflow. As expected, the aroma compound concentration in the product present in the pharynx after

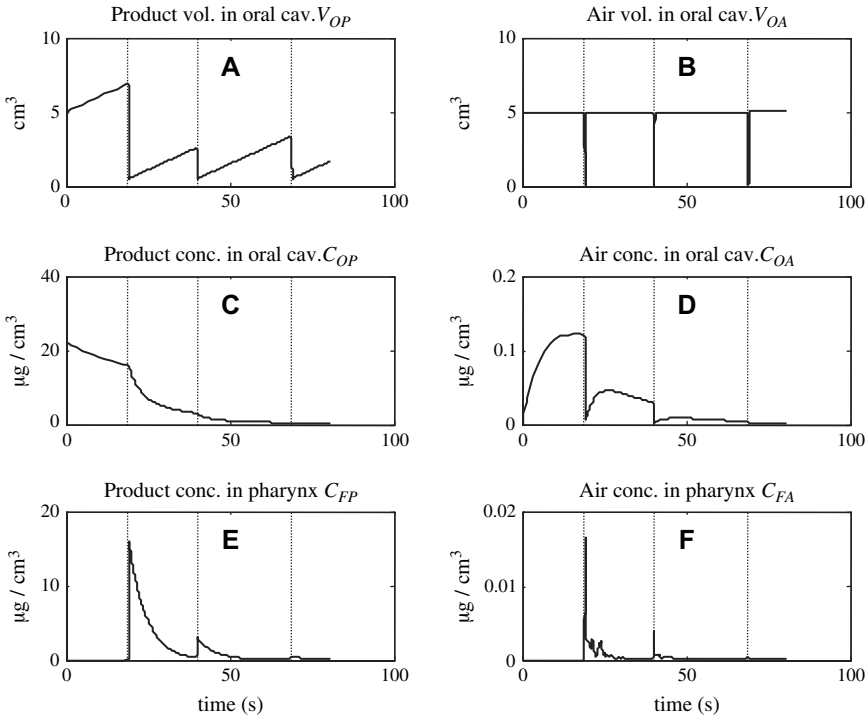

Figure 4 Example of calculated evolutions of volumes and aroma compound concentrations in different compartments. Data for ethyl acetate, yogurt CAS, and panelist A. Simulated values (—) and deglutition events (|). Product (**A**) and air (**B**) volumes in the oral cavity, product (**C**), and air (**D**) concentrations of the volatile compound in the oral cavity, product (**E**), and air (**F**) concentrations of the volatile compound in the pharynx.

each swallowing event is equal to the concentration in the product leaving the oral cavity. The volatile concentration profile in the air contained in the pharynx (C_{FA}) (Figure 4F) is roughly similar to the one in the nasal cavity (Figure 3). However, concentration variations in the pharynx are faster because of a highest dilution effect by the breath airflow, the volume of the pharynx being smaller than that of the nasal cavity.

Imperfect closure of the velopharynx

Velopharynx closure while keeping the product in the mouth can be more or less tight, depending on experiments, on individuals, and on product texture (Buettner et al. 2002). Imperfect closure can result in an additional aroma release from the oral cavity. This phenomenon is mostly visible before the first swallowing event, as illustrated in Figure 5 for panelist C. As the airflow between the oral cavity and the pharynx (Q_{OA}) is assumed to be null during the first step, imperfect closure is represented in the model by a nonzero contact area between the oral cavity and the pharynx. Its evolution with time during the first 12 s of the eating process was represented in the inset in the Figure 5. This contact area can actually account for the observed aroma release to the nasal cavity before the first deglutition (additional release peaks before 12 s in Figure 5B). Yet, comparison of Figures 5A,B reveals that this partial velopharynx opening has relatively little effect on the subsequent release.

Parameter effect on model predictions

The presented mechanistic model contains a large number of parameters, some of which being poorly known, difficult to measure experimentally, and/or subject to significant inter-individual variability. The importance of these parameters for the prediction of the aroma concentration in the nasal cavity was assessed. The goal was to determine those on which future experimental effort should be concentrated in order to improve prediction accuracy and those for which order of magnitude estimations would be sufficient. Each model parameter listed in Table 1 was varied (2-fold decrease or increase). To avoid the masking effect of the relative concentration representation adopted so far, the normalization coefficient used to convert absolute concentrations in the nasal cavity to relative ones was always kept constant when varying any given parameter. As expected, the initial concentration of the aroma compound in the product has a proportional effect on the aroma concentration in the nasal cavity and is not discussed further. Only the most influent model parameters on the nasal aroma concentration are illustrated in Figure 6 and described next.

The reduction of the residual product volume in the pharynx (V_{FP}) accelerates the volatile compound depletion by the breath flow rate (Q_{R}), whereas its increase induces a longer persistence effect (Figure 6A). Variation of the breath flow rate (Q_{R}) has an even strongest but opposite effect, as could be expected: the lowest the breath flow rate, the highest the

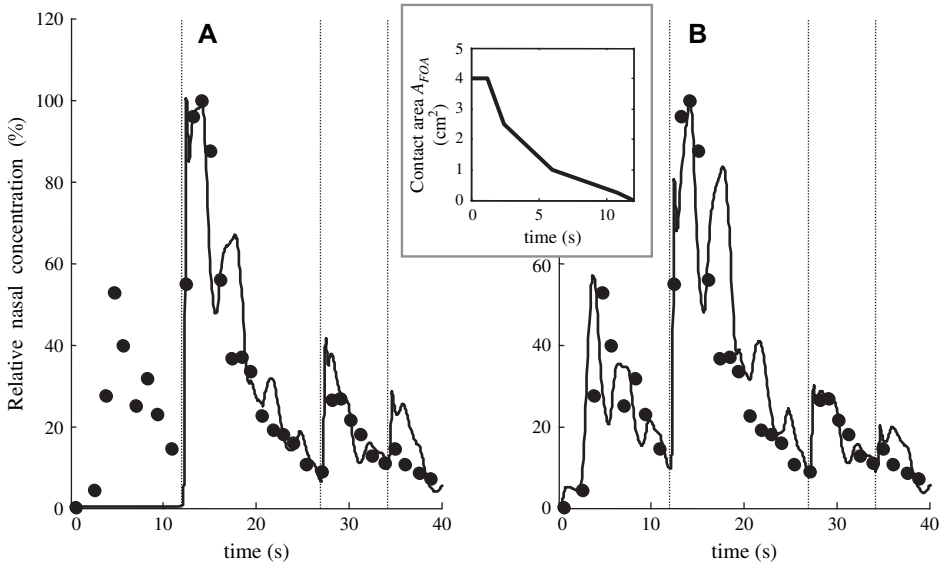

Figure 5 Measured (•) and simulated (—) relative aroma compound concentration in the nasal cavity of panelist C during the consumption of CAS yogurt and deglutition events (|). Simulations of a perfect velopharynx closure (**A**) or a partial velopharynx opening (**B**) while the product is kept in the mouth. Inset: example of a possible time evolution of the contact area between the mouth and the pharynx (A_{FOA}) during the first 12 s of the consumption process when a partial velopharynx opening occurs.

aroma persistence (Figure 6B). The variation of the volume of the nasal cavity (V_{NA}) has a dual effect: a small nasal volume gives high-intensity peaks followed by a quick decrease in the volatile concentration, whereas a large volume gives low intensity peaks but long signal duration (Figure 6C). This double effect results from the combination of an aroma-rich air from the pharynx with aroma-free ambient air in the course of breathing: a lower nasal cavity volume implies higher renewal rate (for the same breath flow Q_R) leading to a quicker increase and decrease. Among all the physicochemical parameters of the aroma/product couple, the most significant effect is obtained for variations in the equilibrium partition coefficient, which represents the volatility of the compound in the matrix being studied (Figure 6D). A 2-fold increase of the partition coefficient (K_{AP}) induces a roughly 1.5-fold increase of the aroma concentration in the nasal cavity, whereas a 2-fold decrease has a symmetrically opposite effect. Similar, but somewhat smallest effects (~1.3-fold increase or decrease) were observed for the contact area between the air and the product in the pharynx (A_{FAP}) and for the mass transfer coefficient in the product (k_P) (data not shown). The volume of the product introduced in the mouth (V_{OPM}) was also found to have a moderate effect, as already noted by Linforth et al. (2005). All other model parameters listed in Table 1, as for example, the contact area between the air and the product in the oral cavity (A_{OAP}) or the mass transfer coefficient in the air k_A, have negligible effect on the simulated nasal aroma concentration, indicating that their accurate knowledge is not essential for running the model. It should be emphasized, however, that these observations are valid for the product, the experimental protocol, the volatile compounds, and the mathematical representation used in this paper. In other situations, the limiting mass transfer phenomena might be different.

Conclusions

The mechanistic approach used in this study allowed the development of an aroma release model describing the consumption process of a food matrix as a succession of steps and including physicochemical as well as physiological parameters. Its fair agreement with experimental in vivo release curves validated the main assumptions that were done concerning involved mechanisms. This study constitutes thus a first step toward accurate prediction of volatile concentration in the nasal cavity of subjects consuming flavored food.

From these bases, several enhancements, concerning the experimental data acquisition or the model accuracy, can be considered. Additional work is required for reliable quantitative measurement of volatile compound concentrations that would allow model validation for absolute rather than relative concentrations. A higher sensitivity spectrometer would be able to measure less-concentrated and/or less-volatile compounds, known to be also important for flavor perception. Measurement of oral concentrations would allow a more complete model validation. A more elaborate processing of the acetone signal and possibly direct measurement of the breath flow rate would improve prediction accuracy because breath flow rate is one of the most sensitive parameters. The consideration of additional phenomena, such as the effect of the product temperature variation and dilution by the saliva on partition and transfer

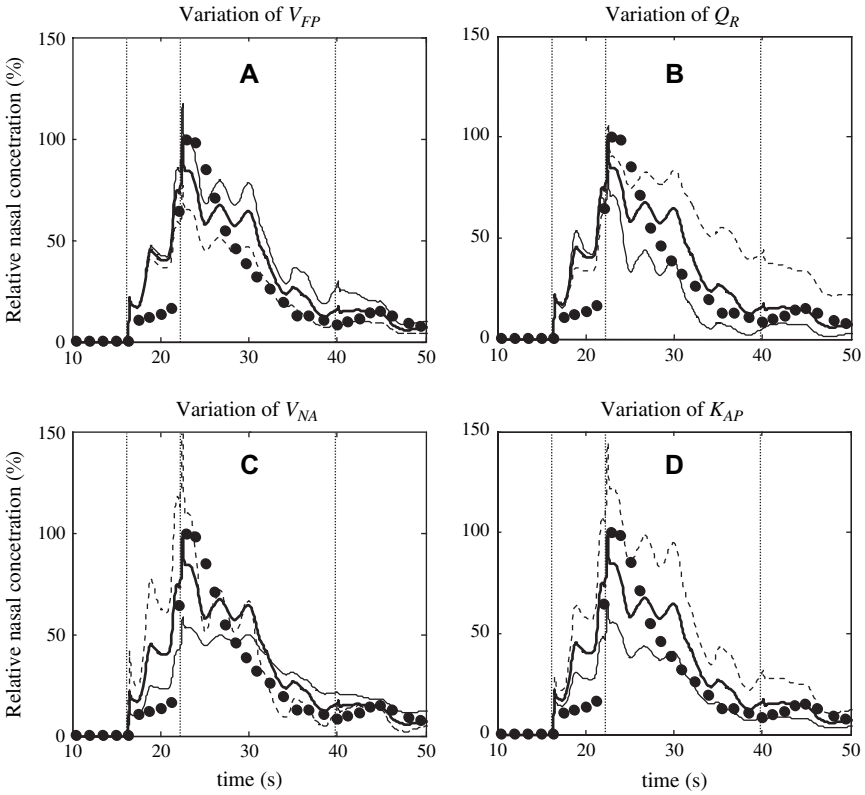

Figure 6 Effect of some of the most sensitive model parameters on the simulated aroma compound concentration in the nasal cavity. Evolution with time of the measured relative ethyl hexanoate concentration in the nasal cavity of panelist B during the consumption of CAS yogurt (•). Variation of the residual product volume in the pharynx V_{FP} (**A**), of the respiration flow rate Q_R (**B**), of the volume of the nasal cavity V_{NA} (**C**), and of the air–product equilibrium partition coefficient K_{AP} (**D**). Simulations were performed with nominal model parameters as given in Table 1 (— bold), with the indicated parameters reduced by a factor of 2 (– –) or increased by a factor of 2 (— thin). Deglutition events (|).

properties of the volatile compounds, should make the simulations even more realistic. Measurements performed on a large number of individuals will enhance the model reliability and possibly allow the definition of classes of consumers, representative of a population. Accurate anatomic and physiological measurements should allow the determination of statistically significant distribution of the most sensitive model parameters among individuals. Finally, model extension to liquid or solid foods would broaden its applicability to many sectors of food industry.

Funding

French government within the framework of the Conception assistée de nouveaux aliments—Intéractions arômes, aliments, emballages project (02P588).

References

Aprea E, Biasioli F, Gasperi F, Mark TD, van Ruth S. 2006. In vivo monitoring of strawberry flavour release from model custards: effect of texture and oral processing. Flavour Fragrance J. 21:53–58.

Atlan S, Trelea IC, Saint-Eve A, Souchon I, Latrille E. 2006. Processing gas chromatographic data and confidence interval calculation for partition coefficients determined by the phase ratio variation method. J Chromatogr A. 1110:146–155.

Bayarri S, Taylor AJ, Hort J. 2006. The role of fat in flavor perception: effect of partition and viscosity in model emulsions. J Agric Food Chem. 54:8862–8868.

Bogaardt HCA, Burger JJ, Fokkens WJ, Bennink RJ. 2007. Viscosity is not a parameter of postdeglutitive pharyngeal residue: quantification and analysis with scintigraphy. Dysphagia. 22:145–149.

Boland AB, Delahunty CM, van Ruth SM. 2006. Influence of the texture of gelatin gels and pectin gels on strawberry flavour release and perception. Food Chem. 96:452–460.

Buettner A, Beer A, Hannig C, Settles M. 2001. Observation of the swallowing process by application of videofluoroscopy and real-time magnetic resonance imaging—consequences for retronasal aroma stimulation. Chem Senses. 26:1211–1219.

Buettner A, Beer A, Hannig C, Settles M, Schieberle P. 2002. Physiological and analytical studies on flavor perception dynamics as induced by the eating and swallowing process. Food Qual Preference. 13:497–504.

Bult JHF, de Wijk RA, Hummel T. 2007. Investigations on multimodal sensory integration: Texture, taste, and ortho- and retronasal olfactory stimuli in concert. Neurosci Lett. 411:6–10.

Collins LMC, Dawes C. 1987. The surface area of the adult human mouth and thickness of the salivary film covering the teeth and oral mucosa. J Dent Res. 66:1300–1302.

Cook DJ, Hollowood TA, Linforth RST, Taylor AJ. 2005. Correlating instrumental measurements of texture and flavour release with human perception. Int J Food Sci Tech. 40:631–641.

Cussler EL. 1997 Diffusion: mass transfer in fluid systems. Cambridge: Cambridge University Press.

Damm M, Vent J, Schmidt M, Theissen P, Eckel HE, Lotsch J, Hummel T. 2002. Intranasal volume and olfactory function. Chem Senses. 27: 831–839.

Dodds WJ. 1989. The physiology of swallowing. Dysphagia. 3:171–178.

Ettre LS, Welter C, Kolb B. 1993. Determination of gas-liquid partition coefficients by automatic equilibrium headspace gas chromatography utilising the phase ratio variation method. Chromatographia. 35:73–84.

Hansson A, Giannouli P, vanRuth S. 2003. The Influence of gel strength on aroma release from pectin gels in a model mouth and in vivo, monitored with proton-transfer-reaction mass spectrometry. J Agric Food Chem. 51:4732–4740.

Harrison M. 1998. Effects of breathing and saliva flow on flavor release from liquid foods. J Agric Food Chem. 46:2727–2735.

Harrison M, Campbell S, Hills BP. 1998. Computer simulation of flavor release from solid foods in the mouth. J Agric Food Chem. 46:2736–2743.

Hiss SG, Treole K, Stuart A. 2001. Effects of age, gender, bolus volume, and trial on swallowing apnea duration and swallow/respiratory phase relationships of normal adults. Dysphagia. 16:128–135.

Hodgson M, Linforth RST, Taylor AJ. 2003. Simultaneous real-time measurements of mastication, swallowing, nasal airflow and aroma release. J Agric Food Chem. 51:5052–5057.

Hodgson M, Parker A, Linforth RST, Taylor AJ. 2004. In vivo studies on the long-term persistence of volatiles in the breath. Flavour Fragrance J. 19:470–475.

Kahrilas PJ, Lin SZ, Logemann JA, Ergun GA, Facchini F. 1993. Deglutitive tongue action—volume accommodation and bolus propulsion. Gastroenterology. 104:152–162.

King BM, Arents P, Bouter N, Duineveld CAA, Meyners M, Schroff SI, Soekhai ST. 2006. Sweetener/sweetness-induced changes in flavor perception and flavor release of fruity and green character in beverages. J Agric Food Chem. 54:2671–2677.

Lauder R, Muhl ZF. 1991. Estimation of tongue volume from magnetic resonance imaging. Angle Orthod. 61:175–184.

Lian G, Malone ME, Homan JE, Norton IT. 2004. A mathematical model of volatile release in mouth from the dispersion of gelled emulsion particles. J Control Release. 98:139–155.

Linforth R, Taylor AJ. 2000. Persistence of volatile compounds in the breath after their consumption in aqueous solutions. J Agric Food Chem. 48:5419–5423.

Linforth RST, Blissett A, Taylor AJ. 2005. Differences in the effect of bolus weight on flavor release into the breath between low-fat and high-fat products. J Agric Food Chem. 53:7217–7221.

Linforth RST, Martin F, Carey M, Davidson J, Taylor AJ. 2002. Retronasal transport of aroma compounds. J Agric Food Chem. 50:1111–1117.

Marin M, Baek I, Taylor AJ. 1999. Volatile release from aqueous solutions under dynamic headspace dilution conditions. J Agric Food Chem. 47:4750–4755.

Netter F. 2004. Atlas d'anatomie humaine. Paris (France): Masson.

Normand V, Avison S, Parker A. 2004. Modelling of the kinetics of flavour release during drinking. Chem Senses. 29:235–245.

Saint-Eve A, Levy C, Martin N, Souchon I. 2006. Influence of proteins on the perception of flavored stirred yogurts. J Dairy Sci. 89:922–933.

Saint-Eve A, Martin N, Guillemin H, Semon E, Guichard E, Souchon I. 2006. Flavored yogurt complex viscosity influences real-time aroma release in the mouth and sensory properties. J Agric Food Chem. 54:7794–7803.

Seta H, Hashimoto K, Inada H, Sugimoto A, Abo M. 2006. Laterality of swallowing in healthy subjects by AP projection using videofluoroscopy. Dysphagia. 21:191–197.

Shaw DW, Williams RBH, Cook IJ, Wallace KL, Weltman MD, Collins PJ, McKay E, Smart R, Simula ME. 2004. Oropharyngeal scintigraphy: a reliable technique for the quantitative evaluation of oral-pharyngeal swallowing. Dysphagia. 19:36–42.

Stephen JR, Taves DH, Smith RC, Martin RE. 2005. Bolus location at the initiation of the pharyngeal stage of swallowing in healthy older adults. Dysphagia. 20:266–272.

Van Loon WAM, Linssen JPH, Boelrijk AEM, Burgering MJM, Voragen AGJ. 2005. Real-time, flavor release from French fries using atmospheric pressure chemical ionization-mass spectrometry. J Agric Food Chem. 53: 6438–6442.

Wilson HK. 1986. Breath analysis. Physiological basis and sampling techniques. Scan J Work Environ Health. 13:174–192.

Wright KM, Hills BP. 2003. Modelling flavour release from a chewed bolus in the mouth: Part II. The release kinetics. Int J Food Sci Tech. 38:361–368.

Wright KM, Hills BP, Hollowood TA, Linforth RST, Taylor AJ. 2003. Persistence effects in flavour release from liquids in the mouth. Int J Food Sci Tech. 38:343–350.

Wright KM, Sprunt J, Smith AC, Hills BP. 2003. Modelling flavour release from a chewed bolus in the mouth: Part I. Mastication. Int J Food Sci Tech. 38:351–360.

Accepted October 18, 2007